Integrated Computer-Aided Engineering 12 (2005) 1–13 1
IOS Press

Performance evaluation of temporal range registration for autonomous vehicle navigation

R. Madhavan* and E. Messina
Intelligent Systems Division, National Institute of Standards and Technology (*NIST*), *Gaithersburg, MD 20899-8230, USA*
Fax: +1 301 990 9688; E-mail: raj.madhavan@ieee.org, elena.messina@nist.gov

Abstract. In this article, we evaluate the performance of an iterative registration algorithm for position estimation of Unmanned Ground Vehicles (UGVs) operating in unstructured environments. Field data obtained from trials on UGVs traversing undulating outdoor terrain is used to quantify the performance of the algorithm in producing continual position estimates. These estimates are then compared with those provided by ground truth to facilitate the performance evaluation of the algorithm. Additionally, we propose performance measures for assessing the quality of correspondences that are crucial to achieving accurate and reliable registration. We describe in detail how these measures, collectively, can provide an indication of the quality of the correspondences thus making the registration algorithm more robust to outliers as spurious matches are not used in computing the incremental transformation.

1. Introduction

Active range sensing has become an integral part of many unmanned vehicle navigation systems due its ability to produce unambiguous, direct, robust, and precise images consisting of range pixels. This is in direct contrast to passive sensing where the inference of range largely remains computationally intensive and not robust enough for use in natural outdoor environments. Depending on the speed of the vehicle, operating environment, and data rate, such range images acquired from a moving platform need to be registered to make efficient use of information contained in them for various navigation tasks including map-building, localization, obstacle avoidance, and control.

Pixel-based methods that attempt to minimize the discrepancies between sensed data and a model of the environment have been utilized for range registration. The attraction of these methods lies in the fact that the matching works directly on data points. Because the search is confined to small perturbations of the range images, it is computationally efficient. For example, Kanade et al. [9] compared elevation maps obtained from 3D range images to determine vehicle location. A similar point matching approach has also been adopted by Shaffer [22]. Cox [4] proposes a point matching method for an indoor robot named Blanche where scan-points from an optical rangefinder are matched to an *a priori* map composed of straight line segments. Blanche's position estimation system utilizes a robust matching algorithm which estimates the precision of the corresponding match/correction that is then optimally combined with odometric position to provide an improved estimate of robot position. Hoffman et al. employ a point matching algorithm for obtaining the inter-frame rotation and translation in a vision-based rover application [6]. Lu [10] finds corresponding points between two successive scans to compute the relative rotation and translation. An Iterative Dual Correspondence algorithm is formulated based on closest point and matching range rules. Olson [20] constructs

*Corresponding author.

ISSN 1069-2509/05/$17.00

a three-dimensional occupancy map of the terrain using stereo vision and iconically matches with a similar map to obtain the relative position between the maps enabling a mobile robot to perform self-localization.

The major drawback of the above approaches is that their use is limited to structured office or factory environments rather than unstructured natural environments. Straightforward correlation-based schemes (for e.g., see [24]), in general, are unable to handle outliers. As cross-correlation calculates the similarity, the two scans must be similar and thus this method cannot accommodate occlusions. This is easy to understand since if areas visible in one scan are not visible in another due to occlusion, then correlation of these scans may produce arbitrarily bad pose (position and orientation) estimates. Also correlation usually places a high burden on computation especially when the scans are at different orientations.

We have developed a temporal iterative algorithm for registering range images obtained from unmanned vehicles. Formally, the process of registration is defined as follows: Given two sets of range images (model set: **M** and data set: **D**), find a transformation (rotation and translation) which when applied to **D** minimizes a distance measure between the two point sets. Despite the apparent simplicity of the problem, to register range images from unmanned vehicles traversing unstructured environments, the terrain of travel, sensor noise, and determination of accurate correspondences make it quite challenging.

The registration algorithm is a modified variant of the well-known Iterative Closest Point (ICP) algorithm [3]. At each iteration, the algorithm determines the closest match for each point and updates the estimated position based on a least-squares metric with some modifications to increase robustness. ICP and its variants have been widely used for registration purposes [21]. For autonomous vehicle navigation, ICP has been used for registration of range images for 3D terrain mapping [7] and localization [13]. Other versions of the ICP algorithm have also been proposed for registration of range images in the presence of outliers [8,19]. Our modified algorithm has been shown to be robust to outliers and false matches during the registration of 3D range images obtained from a scanning LADAR (LAser Detection And Ranging) rangefinder on an Unmanned Ground Vehicle (UGV) and also towards registering LADAR images from the UGV with those from an Unmanned Aerial Vehicle (UAV) that flies over the terrain being traversed [16]. For completeness, the temporal iterative registration algorithm is summarized in Section 2. The modified algorithm is better suited for unstructured environments due to the robustness offered to outliers in the range data that is obtained from sensors aboard UGVs traversing undulating outdoor terrain.

In this article, we evaluate the performance of the registration algorithm for position estimation of UGVs operating in unstructured environments. Field data obtained from two trials on UGVs traversing undulating outdoor terrain is used to quantify the performance of the algorithm in producing continual position estimates. Using the data obtained from the first trial, the iterative registration algorithm aids the position estimation process whenever Global Positioning System (GPS) estimates are unavailable or are below required accuracy bounds. In the second trial, ICP is combined with a post-correspondence Extended Kalman Filter (EKF) to account for uncertainty present in the range images. For both the trials, the position estimates are then compared with those provided by ground truth to facilitate the performance evaluation of the registration algorithm. In addition, we propose performance measures for assessing the quality of correspondences. These measures, collectively, provide an indication of the quality of the correspondences thus making the registration algorithm more robust to outliers as spurious matches are not used in computing the incremental transformation. The registration algorithm is then combined with proposed performance metrics and compared to the traditional ICP algorithm in terms of accuracy and speed.

The article is structured as below: Section 2 describes the modified iterative temporal registration algorithm. Section 3 presents experimental results when the iterative algorithm is used for obtaining position estimates. Section 3.1 compares registration-aided position estimates with those provided by GPS. Section 3.2 details a map-aided registration algorithm for pose estimation. Section 4 develops performance measures for quality assessment of correspondences within the registration process and provides the associated results. Section 5 provides the conclusions and outlines areas of continuing research.

2. Iterative temporal registration algorithm

The process of registration is stated formally as:

$$min_{(\mathbf{R},\mathbf{T})} \sum_i ||\mathbf{M}_i - (\mathbf{R}\mathbf{D}_i + \mathbf{T})||^2 \quad (1)$$

where **R** is the rotation matrix, **T** is the translation vector and the subscript i refers to the corresponding points of the sets **M** and **D**[1].

2.1. Iterative closest point algorithm

The ICP algorithm can be summarized as follows: Given an initial motion transformation between the two point sets, a pair of correspondences are developed between data points in one set and the next. For each point in the first data set, find the point in the second that is closest to it under the current transformation. It should be noted that correspondences between the two point sets is initially unknown and that point correspondences provided by sets of closest points is a reasonable approximation to the true point correspondence. From the pair of correspondences, an incremental motion can be computed facilitating further alignment of the data points in one set to the other. This find correspondence/compute motion process is iterated until a predetermined threshold termination condition.

In its simplest form, the ICP algorithm can be described by the following steps:

1. For each point in data set **D**, compute its closest point in data set **M**. In this article, this is accomplished via nearest point search from the set comprising $N_{\mathbf{D}}$ data and $N_{\mathbf{M}}$ model points.
2. Compute the incremental transformation (**R**,**T**) using Singular Value Decomposition (SVD) via correspondences obtained in step **1.**
3. Apply the incremental transformation from step **2.** to **D**.
4. If relative changes in **R** and **T** are less than a threshold, terminate. Else go to step **1.**

To deal with spurious points/false matches and to account for occlusions and outliers, we modify and weight the least-squares objective function in Eq. (1) such that [25]:

$$\min_{(\mathbf{R},\mathbf{T})} \sum_i w_i \, ||\mathbf{M}_i - (\mathbf{R}\mathbf{D}_i + \mathbf{T})||^2 \qquad (2)$$

If the Euclidean distance between a point x_i in one set and its closest point y_i in the other, denoted by $d_i \triangleq d(x_i, y_i)$, is bigger than the maximum tolerable distance threshold $\mathrm{D}_{\max}$, then w_i is fixed to zero in Eq. (2). This means that an x_i cannot be paired with a y_i since the distance between reasonable pairs cannot be very big. The value of D_{max} is set adaptively in a robust manner by analyzing distance statistics.

Let $\{x_i, y_i, d_i\}$ be the set of original points, the set of closest points and their distances, respectively. The mean and standard deviation of the distances are computed as:

$$\mu = \frac{1}{N}\sum_{i=1}^{N} d_i$$

$$\sigma = \sqrt{\frac{1}{N}\sum_{i=1}^{N}(d_i - \mu)^2}$$

where N is the total number of pairs.

The pseudo-code for the *Adaptive Thresholding* (AT) of the distance D_{max} is given below:

```
if μ < D
D^itn_max = μ + 3σ;
elseif μ < 3D
D^itn_max = μ + 2σ;
elseif μ < 6D
D^itn_max = μ + σ;
else D^itn_max = ε;
```

where itn denotes the iteration number and D is a function of the resolution of the range data. The pseudocode thus provides a procedure for statistically determining D_{max}. Accordingly, the modified algorithm is robust to relatively big motion between the two data sets and to outliers in the data.

During implementation, D was selected based on the following two observations:

1. If D is too small, then several iterations are required for the algorithm to converge and several good matches will be discarded, and
2. If D is too big, then the algorithm may not converge at all since many spurious matches will be included. The interested reader is referred to [25] for more details on the effect and selection of D and ϵ on the convergence of the algorithm.

At the end of this step, two corresponding point sets, $\mathbf{P_M}$:$\{\mathbf{p}_i\}$ and $\mathbf{P_D}$:$\{\mathbf{q}_i\}$ are available.

The incremental transformation (rotation and translation) of step **2.** is obtained as follows [2]:

– Calculate $\mathbf{H}$=$\sum_{i=1}^{N_D}(\mathbf{p}_i - \mathbf{p}_c)(\mathbf{q}_i - \mathbf{q}_c)^T$; ($\mathbf{p}_c$,$\mathbf{q}_c$) are the centroids of the point sets ($\mathbf{P_M}$,$\mathbf{P_D}$).

[1] Though it is not necessary that the model and data sets have the same number of points, after determining correspondences of data points with the model points, the number of model and data points used are the same. Hence only one index is used for both data sets.

– Find the Singular Value Decomposition (SVD) of $\mathbf{H}$ such that $\mathbf{H} = \mathbf{U}\Omega\mathbf{V}^T$ where $\mathbf{U}$ and $\mathbf{V}$ are unitary matrices whose columns are the singular vectors and Ω is a diagonal matrix containing the singular values.
– The rotation matrix relating the two point sets is given by $\mathbf{R} = \mathbf{V}\mathbf{U}^T$.
– The translation between the two point sets is given by $\mathbf{T} = \mathbf{q}_c - \mathbf{R}\mathbf{p}_c$.

This process is iterated as stated in step **4.** until the mean Euclidean distance between the corresponding point sets $\mathbf{P_M}$ and $\mathbf{P_D}$ is less than or equal to a predetermined distance or until a given number of iterations is exceeded.

3. Experimental results of performance evaluation

In this section, we evaluate the performance of the modified ICP algorithm (with adaptive thresholding) using two sets of field trials.

3.1. Registration-aided position estimation

In this section, we estimate the position of an UGV operating in an unknown outdoor environment. The registration algorithm is used for aiding position estimation whenever GPS errors are above a predetermined threshold.[2] Whenever GPS position accuracy falls below the threshold, successive range images are registered with each other from the previous vehicle location (that is either available from dead-reckoning or the previous acceptable GPS estimate) to obtain the current vehicle location.

An Extended Kalman Filter (EKF) was used to fuse encoder, GPS and compass observations to arrive at *ground truth* position estimates. The EKF-based localization algorithm continually corrects the diverging dead-reckoning estimates based on external sensing information provided by GPS and compass corrections. Since the experiments were carried out in an outdoor environment with the UGV executing general motion (translation and rotation on all axes), sensor calibration is especially important to ensure accuracy of readings. For the encoder readings, external sensors (GPS and magnetic compass) were used to obtain calibration factors corresponding to the various axes. The correction factor for magnetic compass was obtained by looking up geodesic charts to determine the angle of magnetic variation corresponding to the longitude/latitude of the experiment's location. It should be noted here that the EKF pose estimate is always superior than that provided by GPS alone and thus has been considered as ground truth. Consequently, a better position fix is guaranteed even when GPS is subject to multipathing errors. The ground truth was obtained in a similar fashion as reported in [15].

Figure 1 shows the results of the position estimation using the registration algorithm. As mentioned earlier, registration of range images is used to aid position estimation when GPS reported positional errors exceed a given threshold. In Fig. 1(a), the registration-aided position estimates are denoted by '$+$' and that of the GPS by '$\circ$'. The wheel encoder estimates are also shown by '$\times$' for comparison. The UGV is subject to slip and skid as a result of the undulatory nature of the terrain of travel. Accordingly, the errors in the wheel encoder estimates grow without bounds. The error between the GPS and the registration-aided position estimates as compared with the ground truth are shown in Fig. 1(b). The solid line represents the error in the registration-aided position estimates and that of the GPS estimate is shown in dashed-dotted line. It is evident that the registration-aided estimates are far superior than that of GPS alone.

3.2. 2D map-aided position estimation

A map-aided position estimation algorithm for computing accurate pose estimates for a UGV operating in tunnel-like environments is described in this section. A bearing-only laser was mounted on the roof of the vehicle so that it could detect strategically placed artificial landmarks (reflective stripes) in the trial environment. The exact position of the landmarks were made available from surveying using a digital theodolite. When the vehicle moves through the environment, the presence of these landmarks is detected by using the observations from the laser. Thus, as the vehicle traverses the environment, a sequence of bearing observations to a number of fixed and known locations are made. Since the locations of these reflectors are known to the vehicle navigation system, the location of the vehicle can be computed from the bearing observations made. Utilizing bearing observations from a bearing-only laser in combination with dead-reckoning sensors (velocity

[2] The error in the GPS positions reported were obtained as a function of the number of satellites acquired. As an alternative, the so-called *dilution of precision* measure associated with the GPS can be used for the same purpose [5].

and steering encoders and rate of change of orientation information from the inertial measurement unit), an EKF was employed to obtain *ground truth* [14]. Using the ground truth together with the information from a range and bearing scanning laser rangefinder, a map of the operating domain, represented by a polyline that adequately approximates the geometry of the environment, is obtained. The map building process relies on position estimation provided by artificial landmarks.

An Iterative Closest Point-Extended Kalman Filter (ICP-EKF) algorithm is used to match range images from a scanning laser rangefinder to the line segments of the polyline map [13]. A compact flowchart that summarizes the algorithm appears in Fig. 2. For this application, ICP alone does not provide sufficiently reliable and accurate vehicle motion estimates. These shortcomings are overcome by combining the ICP with a post-correspondence EKF. Once correspondences are established, a post-correspondence EKF, with the aid of a nonlinear observation model, provides consistent vehicle pose estimates. The observation model relates line segments of the polyline map and range measurements provided by the laser rangefinder enabling the prediction of the range. Using this observation model, it was possible to discard ambiguous range measurements thus increasing the confidence in vehicle position estimates.

The ICP-EKF algorithm has several advantages. First, the uncertainty associated with observations is explicitly taken into account. Second, observations from a variety of different sensors can be easily combined as the changes are reflected only as additional observational states in the EKF. Third, our pixel-based algorithm does not require extraction and matching of features since it works directly on sensed data. Fourth, laser observations that do not correspond to any line segment of the polyline map are discarded during the EKF update stage thus making the algorithm robust to errors in the map.

The estimated vehicle positions (solid line) provided by the ICP-EKF algorithm along with the ground truth (dotted line) is shown in Fig. 3(a).[3] The vehicle travels a distance of 150 meters from right to left. The corresponding 2σ confidence bounds for the absolute error in x, y and ϕ are shown in Fig. 3(b). It can be seen that the errors are bounded and thus the pose estimates are consistent. It is also clear that the estimated path is in close agreement with the ground truth.

[3] As the estimates and their corresponding ground truth are very close, extra effort is required on the part of the reader to distinguish between the two.

4. Performance measures

The correspondence determination process is the most challenging step of the iterative algorithm. Establishing reliable correspondences is extremely difficult as the UGV is subjected to heavy pitching and rolling motion characteristic of travel over undulating terrain. This is further exacerbated by the uncertainty of the location of the sensor platform relative to the global frame of reference. In addition to these factors, noise inherently present in range images complicates the process of determining reliable correspondences.

One solution to overcome the above deficiencies is to extract naturally occurring view-invariant features, for example, corners, from range images. Such *ground control points* can then be used for establishing reliable registration with the ICP algorithm converging to the global minimum. Towards registering LADAR images from a UGV with those from an Unmanned Aerial Vehicle (UAV) that flies over the terrain being traversed, we have developed a hybrid registration approach. In this approach to air to ground registration to estimate and update the position of the UGV, we register range data from two LADARs by combining a feature-based method with the modified ICP algorithm. Registration of range data guarantees an estimate of the vehicle's position even when only one of the vehicles has GPS information. Temporal range registration enables position information to be continually maintained even when both vehicles can no longer maintain GPS contact. The feature-based hybrid approach was shown to be effective in producing reliable registration for UGV navigation in rugged terrain and urban environments using real field data acquired from two different LADARs on the UGV [16].

For the map-aided position estimation scheme described in Section 3.2, the ICP-EKF algorithm failed to produce unambiguous correspondences with the map whenever variations in data sets were not unique. To enable ICP to produce accurate correspondences, a strategy to augment the ICP-EKF algorithm with artificial/natural landmarks was devised to provide external aiding. To facilitate the selection of landmarks, an entropy-based metric was developed to enable the evaluation of information contained in a potential landmark. A curvature scale space algorithm was developed to extract natural landmarks from laser rangefinder scans [12]. The proposed landmark augmentation methodology has been verified for the localization of a Load-Haul-Dump truck and resulted in the

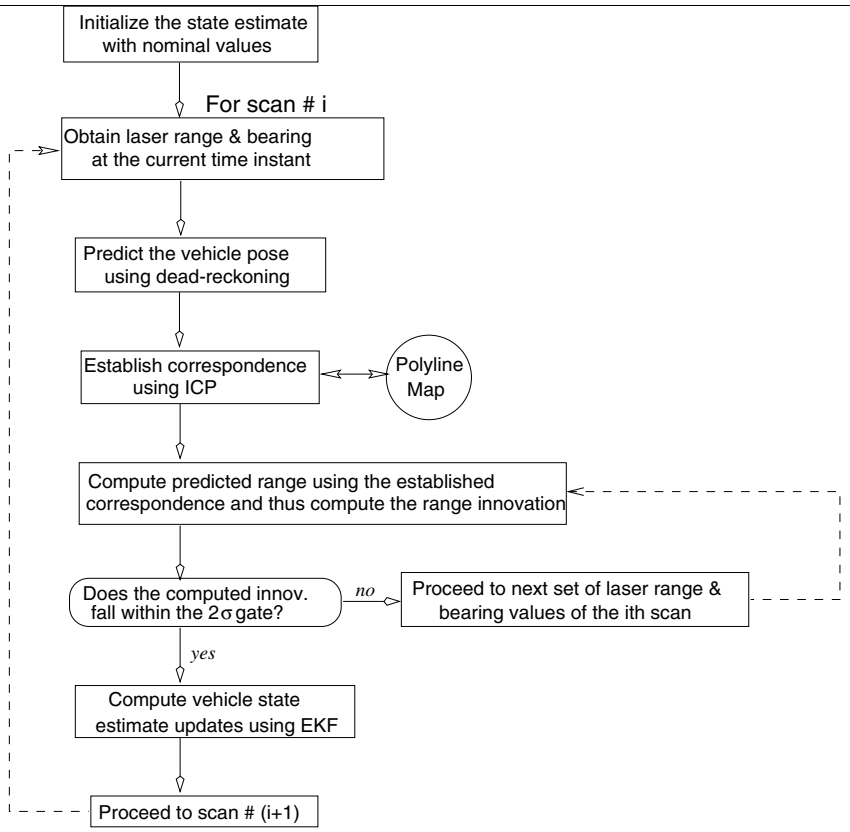

Fig. 2. Flowchart of the ICP-EKF algorithm.

ICP-EKF algorithm producing reliable and consistent estimates [13].

We propose the following measures towards performance evaluation of the registration algorithm for position estimation.

4.1. ICP estimate and dead-reckoning prediction measure

The ICP itself can be used to compute the estimates of the pose of the UGV. This can be compared with dead-reckoning estimates each time before the correspondences are computed. More specifically, the prediction covariance (from dead-reckoning) can be utilized as a check on the ICP estimates, since if the associated state covariances become large, this is an indication of the state estimation filter divergence as a result of the poor ICP estimates.

The largest Eigenvalue of the predicted state covariance matrix (that is a measure of the total positional uncertainty) can be used as a measure to check the quality of the ICP estimates. Also the determinant of the predicted state covariance matrix can be used as a measure since it represents total predicted uncertainty and this can be observed to see if the ICP produces reliable and non-divergent estimates (since once the ICP estimates start behaving erratically, this is reflected by similar behavior in the correspondences).

4.2. Mean squared error measure

To indicate if the correspondences make sense the following measure is proposed:

$$\mathrm{P}_{mse} = \frac{1}{n}\sum_{i=1}^{n}\left[d\left(p_i, \ell_i\right)\right]^2$$

where p_i and ℓ_i are the i^{th} of n range data points and $d\left(p_i, \ell_i\right)$ is the distance from the p_i^{th} point to the ℓ_i^{th} point. Global minimum of the function will occur at the *true* pose of the vehicle.

At the true pose, all or at least the majority of the range data points will be close to their corresponding points, thus yielding a very low value for the correct solution. The problem with this measure is that it is

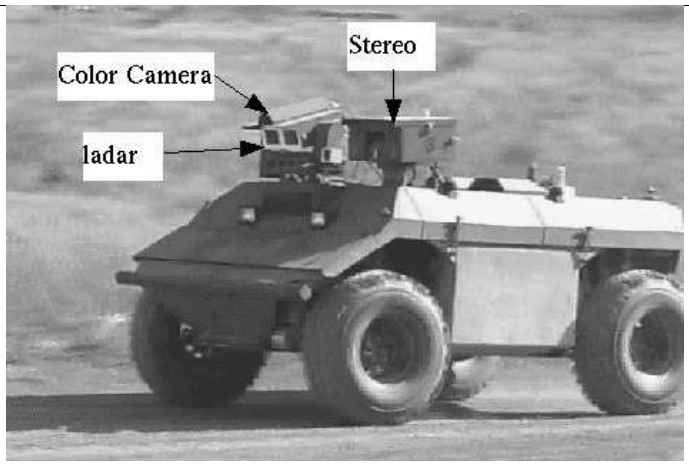

Fig. 4. The UGV used for field trials is a Demo III [23] eXperimental Unmanned Vehicle (XUV). It is a hydrostatic diesel, 4 wheel drive, 4 wheel steer vehicle and can autonomously navigate at 60 km/h on-road and at 35 km/h off-road in daylight, and 15 km/h off-road at night or under inclement weather conditions. The vehicle employs the NIST developed 4D/RCS (Real-Time Control System) [1] for autonomous navigation. The primary navigation suite of this vehicle consists of a LADAR, color cameras, Global Positioning System (GPS), and an Inertial Navigation System (INS).

difficult to decide if the pose is true in the presence of outliers and occlusions.

4.3. Classification factor

Similar to [11], we define *well defined data points* as those points that lie within some distance threshold from their corresponding points:

$$\mathrm{P}_{cf} = \frac{1}{n} \sum_{i=1}^{n} \left(1 - \frac{d^m}{d^m + c^m} \right)$$

where $d = d\left(p_i, \ell_i\right)$, $c =$ neighborhood size, $m =$ sigmoid steepness. The sigmoid function has a value close to unity when the data points are closer to their corresponding points and a value close to zero for those that are farther. The value of c depends on the data under consideration, particularly the sensor error. The chosen value of c effectively weights the closer points heavily and vice-versa. Thus, this measure rejects outliers and provides an added degree of robustness.

At true pose, global maximum should approach close to unity and will be less in the neighborhood of well defined data points. Note that P_{cf} values can fall only between [0,1]. In addition, this measure indirectly indicates the *future-goodness* of the pose estimate if a certain threshold is exceeded. The problem with this measure could be that it is not as sensitive as P_{mse} since it applies only for a certain local neighborhood. Thus P_{mse} can be used as a comparative performance measure whereas P_{cf} for pass/fail decisions for the correspondences before they are passed on for computing the incremental transformation.

4.4. Comparative performance measure

It is the ratio defined by

$$\mathrm{P}_{cpm} = \frac{{\mathrm{P}_{cf}}^2}{\mathrm{P}_{mse}}$$

The peak of this measure should occur at the true pose. In other words, this measure serves as a nonlinear scaling factor applied to the inverse of the measure, P_{mse}.

4.5. Results and discussion

In this section, we use 3D LADAR data obtained during field trials to illustrate the utility of the proposed metrics in assessing the quality of correspondences. For details on the quantification of the performance, additional results, and real-time implementation issues of the iterative registration algorithm, the interested reader is referred to [17].

The LADAR was mounted on a UGV traversing rugged terrain on a pan/tilt platform to increase its narrow 20° field of view. The UGV (shown in Fig. 4) traversed vegetated and rugged terrain during the course of the field trials experiencing heavy pitching and rolling motion characteristic of travel over such undulating terrain. The range of the tilt motion is $\pm 30^\circ$ resulting in an effective field of view of about 90° and providing a range image of 32 lines $\times$ 180 pixels where each data point contains the distance to a target in the operating environment. The angular resolution of this LADAR is

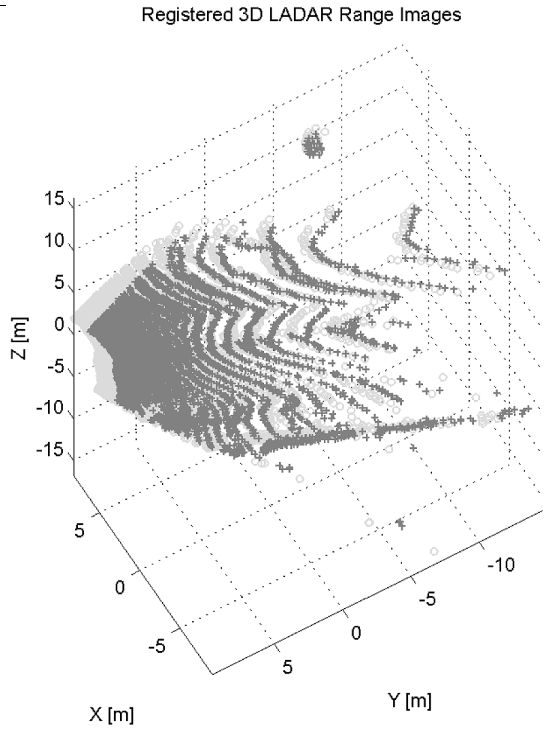

(a) Direct ICP

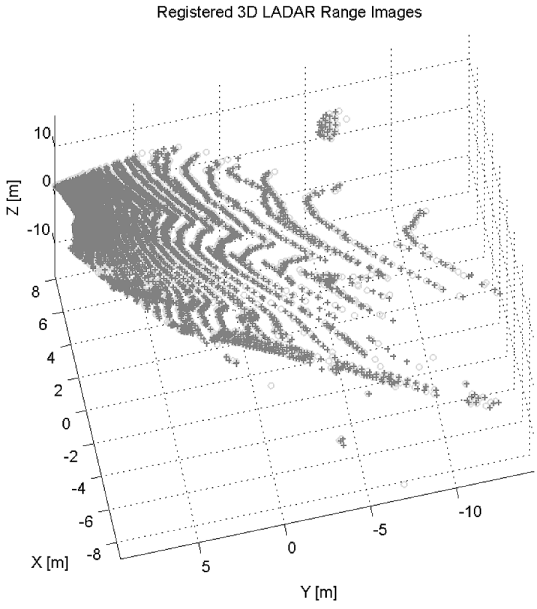

(b) Modified ICP with AT and $\mathcal{P}_{mse}$

Fig. 5. Illustration of 3D LADAR registration via the direct (w/o AT and $\mathcal{P}_{mse}$) and combined ICP algorithms. The model ('$\circ$') and data ('$+$') points before (a) and after (b) registration are shown.

$0.658^\circ \times 0.5^\circ$ in the horizontal and vertical directions, respectively. Utilizing knowledge about the LADAR mount position and calibration factors, the range information provided by the LADAR is transformed to cartesian coordinates.

We illustrate the combined utility of adaptive thresh-

olding and the P_{mse} measure by using it to register 3D range images. We then compare the registration results with direct ICP (i.e., without AT and P_{mse}). For the comparison, the same termination threshold condition is employed for both the algorithms.

Figures 5 and 6 summarize the comparative results. Figures 5(a) and 6(b) show the registered LADAR images via the direct and combined ICP algorithms, respectively. The combined ICP needed 39 iterations whereas the direct ICP took 82 iterations and the mean distances before and after registration were 0.07 m and 0.19 m for the two algorithms, respectively. Figures 6(a) and 6(b) show the closest point distance before and after registration. It is thus evident that the combined ICP algorithm is vastly superior than the direct ICP algorithm both in terms of accuracy and speed. Even though the P_{mse} metric is sensitive to outliers, we contend that the adaptive thresholding methodology in combination with the mean-squared error metric provides an acceptable means in inferring the validity of the position estimate.

5. Conclusions and further work

The evaluation of performance of an iterative registration algorithm for position estimation of UGVs operating in unstructured environments was the main theme of this article. A modified ICP algorithm was used to aid the position estimation process and the resulting estimates were compared with ground truth to facilitate the performance evaluation for two sets of field data. Field data obtained from trials on UGVs traversing undulating outdoor terrain was used to quantify the performance of the algorithm in producing continual position estimates.

In the first set of experimental results, registration-aided position estimates were generated whenever GPS estimates were unavailable or unreliable. For the second set of trials, the ICP-EKF algorithm was used for map-aided position estimation. In both cases, the presented results demonstrated the efficacy of the registration algorithm for position estimation.

Performance measures towards assessing the quality of correspondences required for accurate and efficient registration were developed in the second part of the article. The modified algorithm was combined with the mean-squared error metric to register 3D LADAR range images. The combined algorithm was then evaluated against the direct ICP algorithm. The accompanying results showed the superiority of the combined algorithm both in terms of speed and accuracy.

P_{cf} and P_{cpm} have not been used in the results presented in this article. The combination of AT and P_{mse} offer robustness to false correspondences and thus result in a reduced number of iterations. We also expect that there will be intra-iterative advantages not only with efficient correspondences but also with respect to the overall quality of the incremental transformation. Quantitative evaluation of these issues remain as candidates of continuing research.

Future work includes combining the measures to achieve efficient 3D registration for mapping and position estimation tasks, both in indoor and outdoor environments. Currently, we are in the process of obtaining LADAR data in areas where GPS accuracy degrades and then approaches its best estimate. Such data sets would be of immense value in evaluating the utility of the registration algorithm and the proposed performance measures.

References

[1] J. Albus et al., *4D/RCS Version 2.0: A Reference Model Architecture for Unmanned Vehicle Systems*, Technical Report NISTIR 6910, National Institute of Standards and Technology, 2002.

[2] K. Arun, T. Huang and S. Blostein, Least-Squares Fitting of Two 3-D Point Sets, *IEEE Transactions on Pattern Analysis and Machine Intelligence* **9**(5) (1987), 698–700.

[3] P. Besl and N. McKay, A Method for Registration of 3-D Shapes, *IEEE Transactions on Pattern Analysis and Machine Intelligence* **14**(2) (1992), 239–256.

[4] I. Cox, BLANCHE – An Experiment in Guidance and Navigation of an Autonomous Robot Vehicle, *IEEE Transactions on Robotics and Automation* **7**(2) (1991), 193–204.

[5] M.S. Grewal, L.R. Weill and A.P. Andrews, *Global Positioning Systems*, Inertial Navigation and Integration. Wiley, 2001.

[6] B. Hoffman, E. Baumgartner, T. Huntsberger and P. Schenker, Improved Rover State Estimation in Challenging Terrain, *Autonomous Robots* **6**(2) (April, 1999), 113–130.

[7] D. Huber, O. Carmichael and M. Hebert, *3D Map Reconstruction from Range data*, in Proceedings of the IEEE International Conference on Robotics and Automation, 2000, 891–897.

[8] V. Koivunen, J. Vezien and R. Bajcsy, *Multiple Representation Approach to Geometric Model Construction from Range Data*, Technical Report MS-CIS-93-66, GRASP Lab., University of Pennsylvania, 1993.

[9] I. Kweon and T. Kanade, High Resolution Terrain Map from Multiple Sensor Data, *In Proceedings of the IEEE International Workshop on Intelligent Robots and Systems* **1** (1990), 127–134.

[10] F. Lu, *Shape Registration using Optimization for Mobile Robot Navigation*, PhD thesis, Dept. of Computer Science, University of Toronto, 1995.

[11] P. MacKenzie and G. Dudek, *Precise Positioning using Model-based Maps*, in Proceedings of the IEEE International Conference on Robotics and Automation, 1994, 1615–1621.

[12] R. Madhavan and H. Durrant-Whyte, Natural Landmark-based Autonomous Navigation using Curvature Scale Space, *Robotics and Autonomous Systems* **46**(2) (February, 2004), 79–95.

[13] R. Madhavan and H. Durrant-Whyte, Terrain Aided Localization of Autonomous Ground Vehicles, *Special Issue of the Journal of Automation in Construction* (*Invited*) **13**(1) (January, 2004), 69–86.

[14] R. Madhavan et al., *Evaluation of Internal Navigation Sensor Suites for Underground Mining Vehicle Navigation*, In Proceedings of the IEEE International Conference on Robotics and Automation, May, 1999, 999–1004.

[15] R. Madhavan, K. Fregene and L.E. Parker, Distributed Cooperative Outdoor Multi-robot Localization and Mapping, *Autonomous Robots: Special Issue on Analysis and Experiments in Distributed Multi-Robot Systems* **17**(1) (July, 2004), 23–39.

[16] R. Madhavan, T. Hong and E. Messina, *Temporal Range Registration for Unmanned Ground and Aerial Vehicles*, in Proceedings of the IEEE International Conference on Robotics and Automation, April, 2004, 3180–3187.

[17] R. Madhavan and E. Messina, *Iterative Registration of 3D LADAR Data for Autonomous Navigation*, in Proceedings of the IEEE Intelligent Vehicles Symposium, June, 2003, 186–191.

[18] R. Madhavan and E. Messina, *Quantifying Uncertainty Towards Information-Centric Unmanned Navigation*, in Proceedings of the Performance Metrics for Intelligent Systems Workshop, September 2003. Available from http://www.isd.mel.nist.gov/PerMIS_2004/Past.htm.

[19] T. Masuda and N. Yokoya, *A Robust Method for Registration and Segmentation of Multiple Range Images*, in Proceedings of the Second IEEE CAD-based Vision Workshop, 1994, 106–113.

[20] C. Olson, Probabilistic Self-Localization for Mobile Robots, *IEEE Transactions on Robotics and Automation* **16**(1) (February, 2000), 55–66.

[21] S. Rusinkiewicz and M. Levoy, *Efficient Variants of the ICP Algorithm*, in Proceedings of the International Conference on 3-D Digital Imaging and Modeling, 2001, 145–152.

[22] G. Shaffer, *Two-Dimensional Mapping of Expansive Unknown Areas*, PhD thesis, Carnegie Mellon University, 1992.

[23] C. Shoemaker and J. Bornstein, *The Demo III UGV Program: A Testbed for Autonomous Navigation Research*, in Proceedings of the IEEE ISIC/CIRA/ISAS Joint Conference, September, 1998, 644–651.

[24] G. Weiβ, C. Wetzler and E. von Puttkamer, *Keeping Track of Position and Orientation of Moving Indoor Systems by Correlation of Range-finder Scans*, in Proceedings of the IEEE/RSJ International Conference on Intelligent Robots and Systems, (Vol. 1), September, 1994, 595–601.

[25] Z. Zhang, Iterative Point Matching for Registration of Free-Form Curves and Surfaces, *International Journal of Computer Vision* **13**(2) (1994), 119–152.

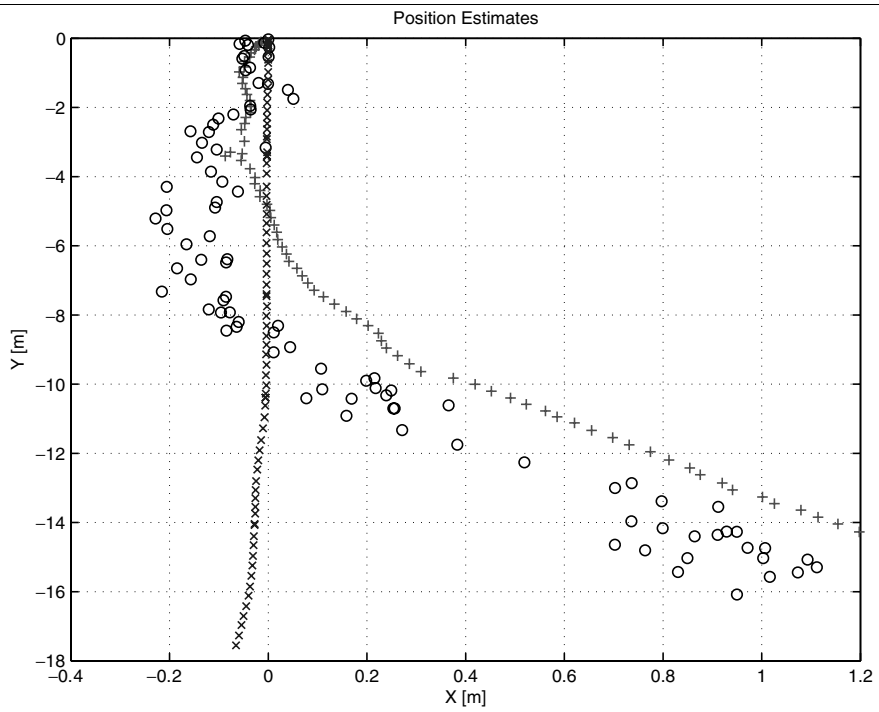

(a)

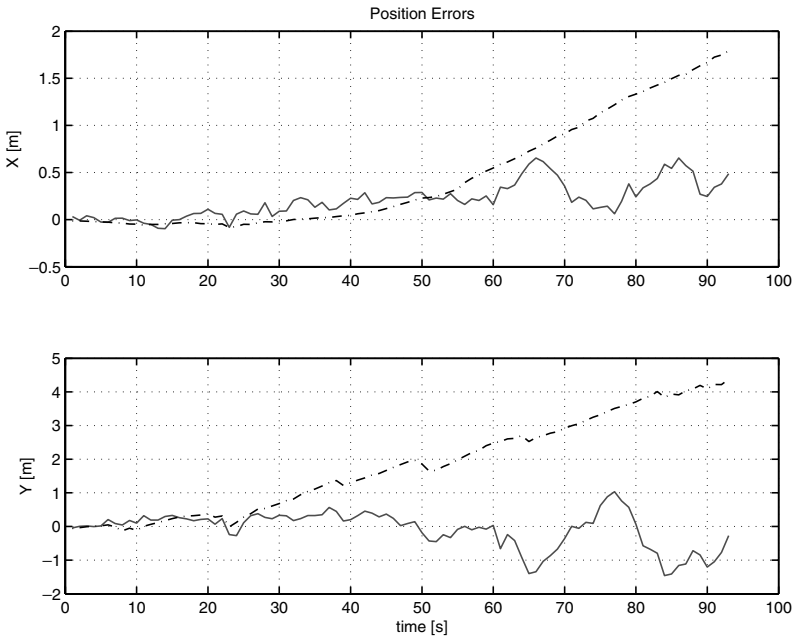

(b)

Fig. 1. Registration-aided position estimation. The aided estimates are shown by '+' and that of GPS by '○'. The wheel encoder estimates shown by '×' are included for comparison in (a). In (b), position errors as compared to the ground truth is depicted; the solid line represents the error in the registration-aided position estimates and that of the GPS estimate is shown in dashed-dotted line.

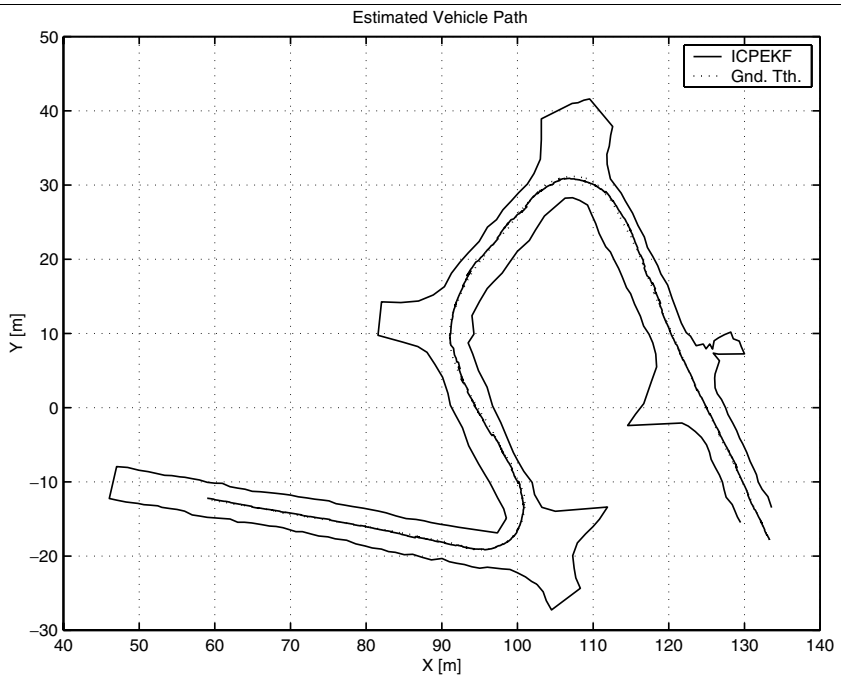

(a)

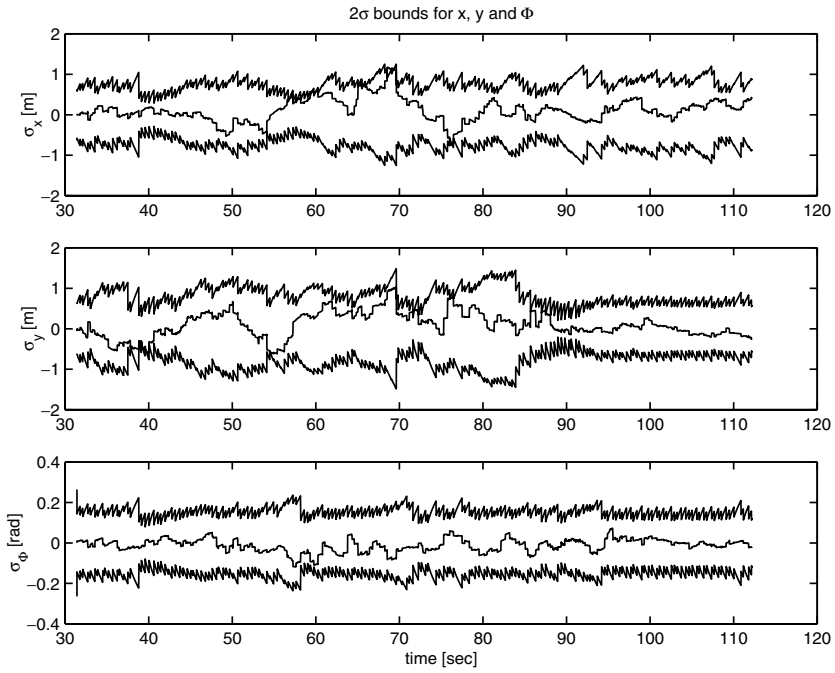

(b)

Fig. 3. 2D Map-aided Position Estimation. ICP-EKF estimated position the trial vehicle (solid line) and the ground truth (dotted line) are shown in (a). The 2σ confidence bounds are computed using the covariance estimate for the error in x, y and ϕ compared to the actual error computed with the ground truth estimates as depicted in (b).

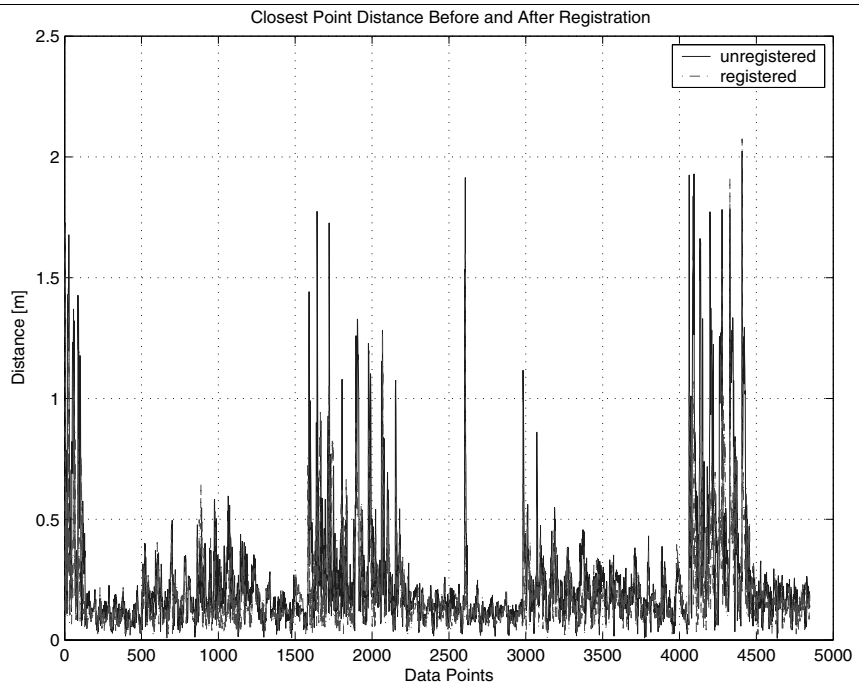

(a)

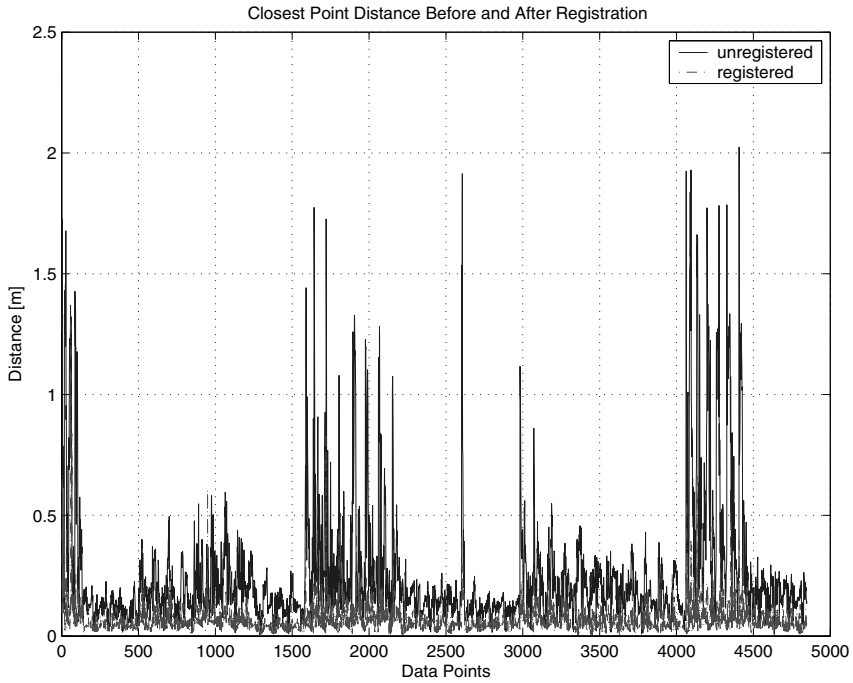

(b)

Fig. 6. The registered (shown in dashed-dotted line) and unregistered (shown in solid line) closest point distances are shown corresponding to the registration of range images depicted in Figs 5(a) and 5(b), respectively. (a) and (b) show the closest point distances via the direct ICP (w/o AT and P_{mse}) and the combined ICP algorithms, respectively.